Knut Waagan. Mapping low frequency blast noise using a numerical weather forecast. Proceedings of the 38th Scandinavian Symposium on Physical Acoustics, Geilo 30 February 2 - 6, 2013. Editor: Rolf J. Korneliussen, ISBN 978-82-8123-015-6.

MAPPING LOW FREQUENCY BLAST NOISE USING A NUMERICAL WEATHER FORECAST

Knut Waagan

Forsvarets Forskningsinstitutt
Instituttveien 20
2007 Kjeller

Abstract

We consider long ranging acoustic noise in the band 1-100 Hz, motivated by the need to model low frequency sound propagation around Norwegian shooting ranges. A wide-angle parabolic approximation is used with meteorological input from a numerical weather forecasting model. Simplified representations of the weather data are also used as input, and we find that they can have predictive value, although details may be lost. Up to at least a few km away from the source, our results indicate that surface layer modelling is important. Downward refracting conditions quite high up in the atmosphere are shown to be important at long distances, which limits the predictive value of near-ground observations.

1 Introduction

In areas surrounding military shooting ranges, acoustic low frequency noise can cause annoyance over large ranges, at least up to 10-20 km. At such ranges, atmospheric conditions strongly influence the received sound levels. Obtaining and interpreting meteorological data is hence crucial for predicting noise with numerical methods. In this study, we consider meteorological data taken directly from a numerical weather forecasting code. Our motivation is two-fold: To demonstrate the ability of a new propagation code to handle realistic data, and to gain some insight into the predictability of noise levels. It must be noted that the realism of the weather forecast data is limited by numerical resolution and modelling assumptions. In particular, the topography is smeared out, and smaller scale flow features are absent.

1.1 Propagation algorithm

Sound propagation was modelled with a wide-angle parabolic equation. The Claerbout approximation was used. Weather data were incorporated via the effective sound speed, i.e. the thermal sound speed plus the wind component in the horizontal propagation direction. Topography was included using the GTPE approach ([4]), which uses height above ground as the vertical coordinate. More details on our implementation can be found in [5] and in a technical report to appear soon.

An impedance boundary condition was imposed. The ground impedance data were taken from NGI ground classification in [2], where the poroelastic Multipor model ([3]) was used to assign impedance values. This yielded a rather soft ground except for some small water features. The impedance boundary condition does not allow dependence on incidence angle, hence we used grazing angle values of impedance.

For completeness, some numerical parameter choices should be stated: The range resolution of the input data was fixed to 25 m during the simulation. This was a conservative choice; Using larger range-independent chunks would quite possibly be more efficient. The Crank-Nicolson method was used to integrate the parabolic equation with grid size one tenth of a wavelength vertically as well as horizontally. The computational domain was truncated at 2.5 km above ground and an absorption layer 50 wavelengths thick was used to suppress reflections. the maximum range was taken to be 25 km. On a desktop computer, we simulated the band 1-100 Hz with 12th octave frequency resolution in about 8 minutes, while on our laptop it took about 12 minutes.

1.2 Weather forecast data

We considered a snapshot from the Arome model weather forecast, which was provided by the Norwegian Meteorological Institute. We used [1] as a reference for interpreting the data. The snapshot consisted of a transect from east to west crossing a military training facility. Resolution was as presently used in the numerical weather forecast: Horizontally, there are 2.5 km between grid points. The vertical resolution decreases with height, with the lowest grid point about ten metres above ground. So called σ-coordinates are used, such that the grid follows the topography near ground and the isopressure curves higher up.

Weather data from the snapshot are plotted in Figure 1.1. We show temperature and the horizontal wind component in the transect direction. The temperature field was largely horizontal, and decreasing with height. The wind was from the east and showed significant range variation. There was a jet around 1000 m altitude, above which the wind decreased. In sound prediction, it is common to use simplified models of the atmosphere, hence we wanted to study the effect of simplifying the forecast data. As an example, we employed a curve fit as illustrated in Figure 1.2. In this figure, wind and temperature values (from the Arome grid points) are plotted against altitude. Least Squares polynomial fits are shown, resulting in weather profiles that only depend on altitude. We refer to these profiles as range-independent curve fits in the following.

In Figure 1.1, one can observe a kind of surface layer; The wind field tapered off near the ground surface. Using the range-independent curve fit might therefore underestimate

Knut Waagan. Mapping low frequency blast noise using a numerical weather forecast. Proceedings of the 38th Scandinavian Symposium on Physical Acoustics, Geilo 30 February 2 - 6, 2013. Editor: Rolf J. Korneliussen, ISBN 978-82-8123-015-6.

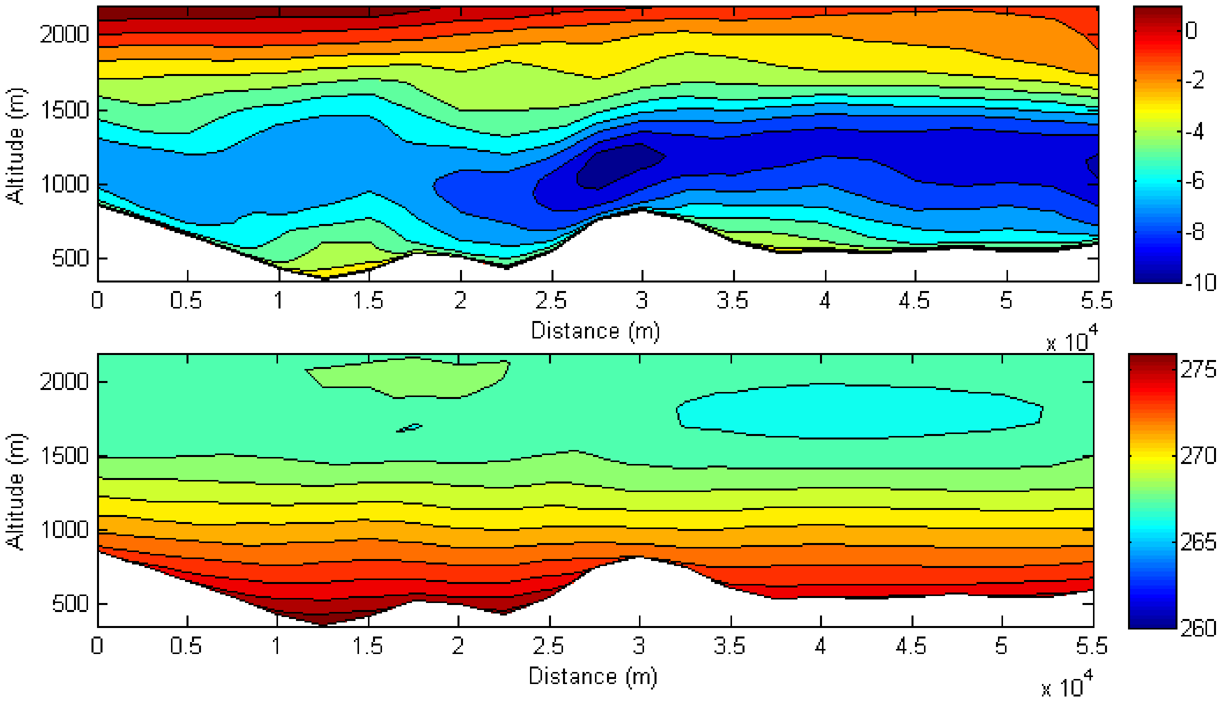

Figure 1.1: *Top: Horizontal wind component along transect (m/s). Bottom: Temperature (K).*

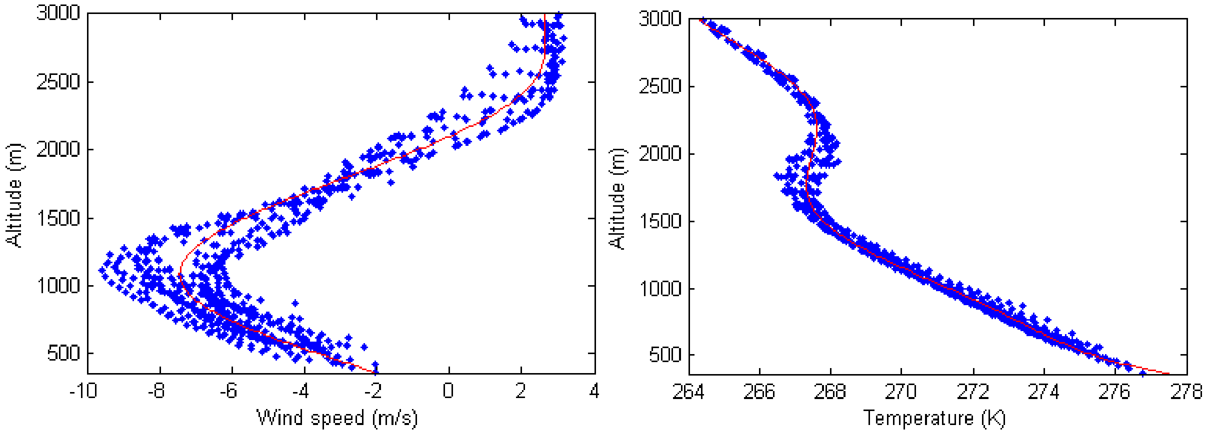

Figure 1.2: *Fitted profiles and data points for wind speed (left) and temperature (right).*

Knut Waagan. Mapping low frequency blast noise using a numerical weather forecast. Proceedings of the 38th Scandinavian Symposium on Physical Acoustics, Geilo 30 February 2 - 6, 2013. Editor: Rolf J. Korneliussen, ISBN 978-82-8123-015-6.

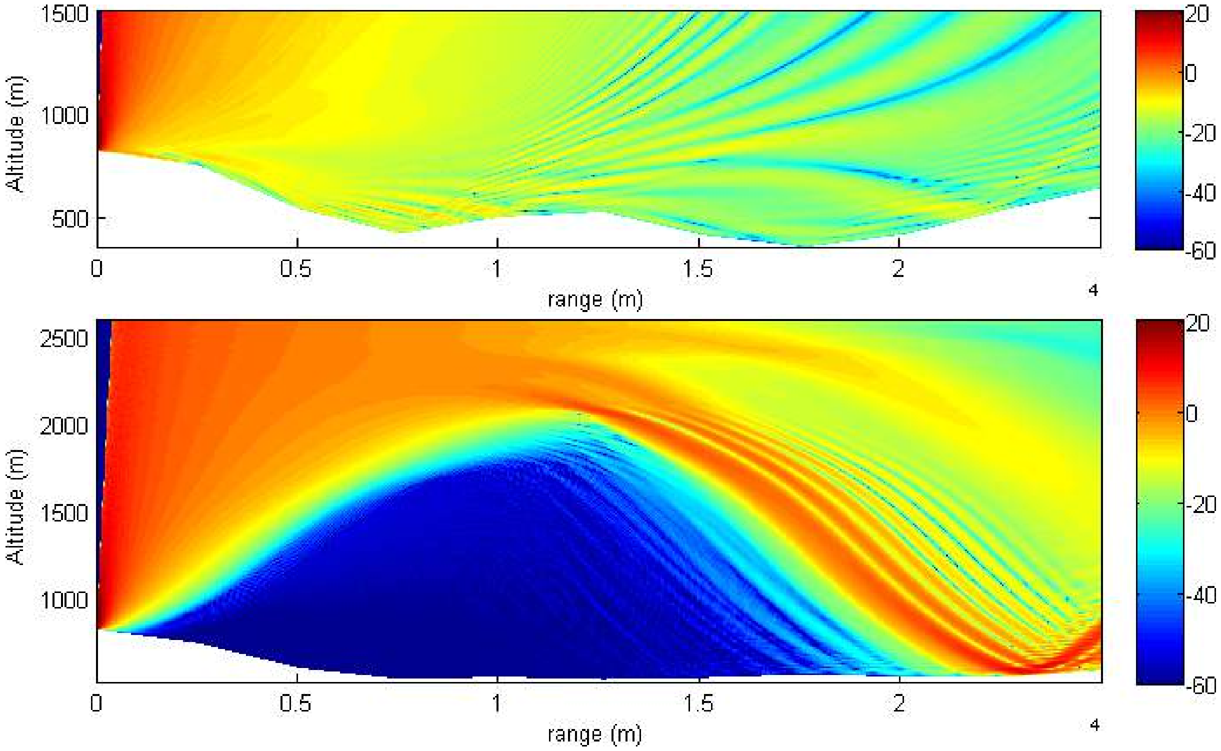

Figure 2.1: *Relative sound level at 64 Hz. Top: Westwards (downwind) propagation. Bottom: Eastwards (upwind) propagation.*

the effective sound speed gradient near the ground. To compensate we tried to scale the wind with a taper function near the ground. We chose the logarithmic taper

$$s(\xi) = \min[1, \ln(\xi/\xi_0 + 1)/\ln(\xi_1/\xi_0 + 1)],$$

where ξ denotes height above ground. Such a shape is commonly used to model wind in the surface layer. We found that a 'roughness length' $\xi_0 = 0.5$ m and a cutoff height $\xi_1 = 100$ m gave a reasonable looking approximation.

Effective sound speed for the PE computational grid was derived from the Arome data as follows: Between the Arome grid points, the effective sound speed was interpolated bilinearly. Below the Arome grid we extrapolated temperature linearly from above, while we set the wind speed to zero at the surface, and then interpolated linearly. A lin-log type wind profile between the surface and the Arome grid was also tried, but had limited impact on the results.

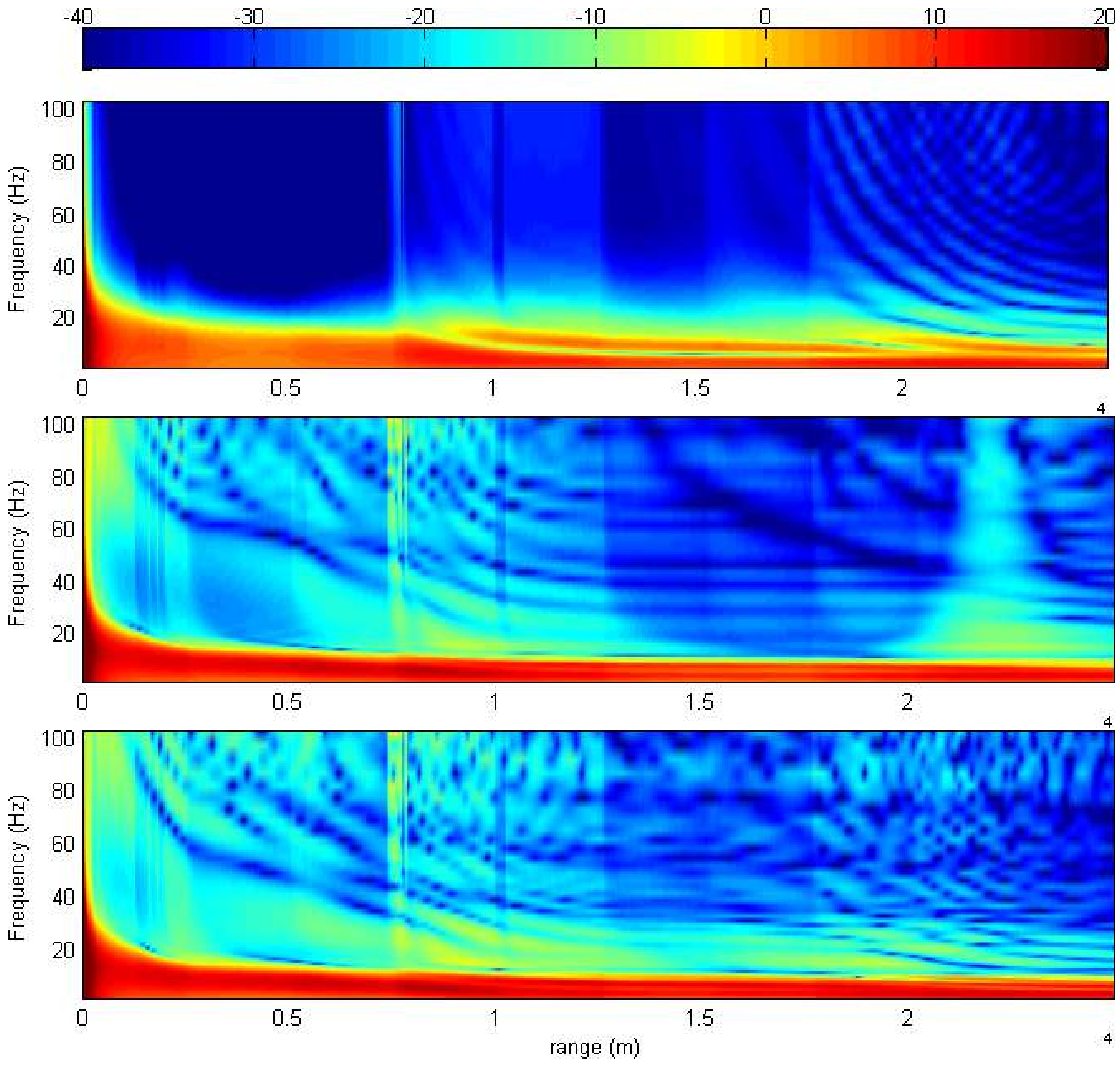

Figure 2.2: *Relative sound level as a function of range and frequency. Westwards propagation. Top: Curve fitted profile. Middle: Full data set. Bottom: Curve fitted profile with surface taper.*

Knut Waagan. Mapping low frequency blast noise using a numerical weather forecast. Proceedings of the 38th Scandinavian Symposium on Physical Acoustics, Geilo 30 February 2 - 6, 2013. Editor: Rolf J. Korneliussen, ISBN 978-82-8123-015-6.

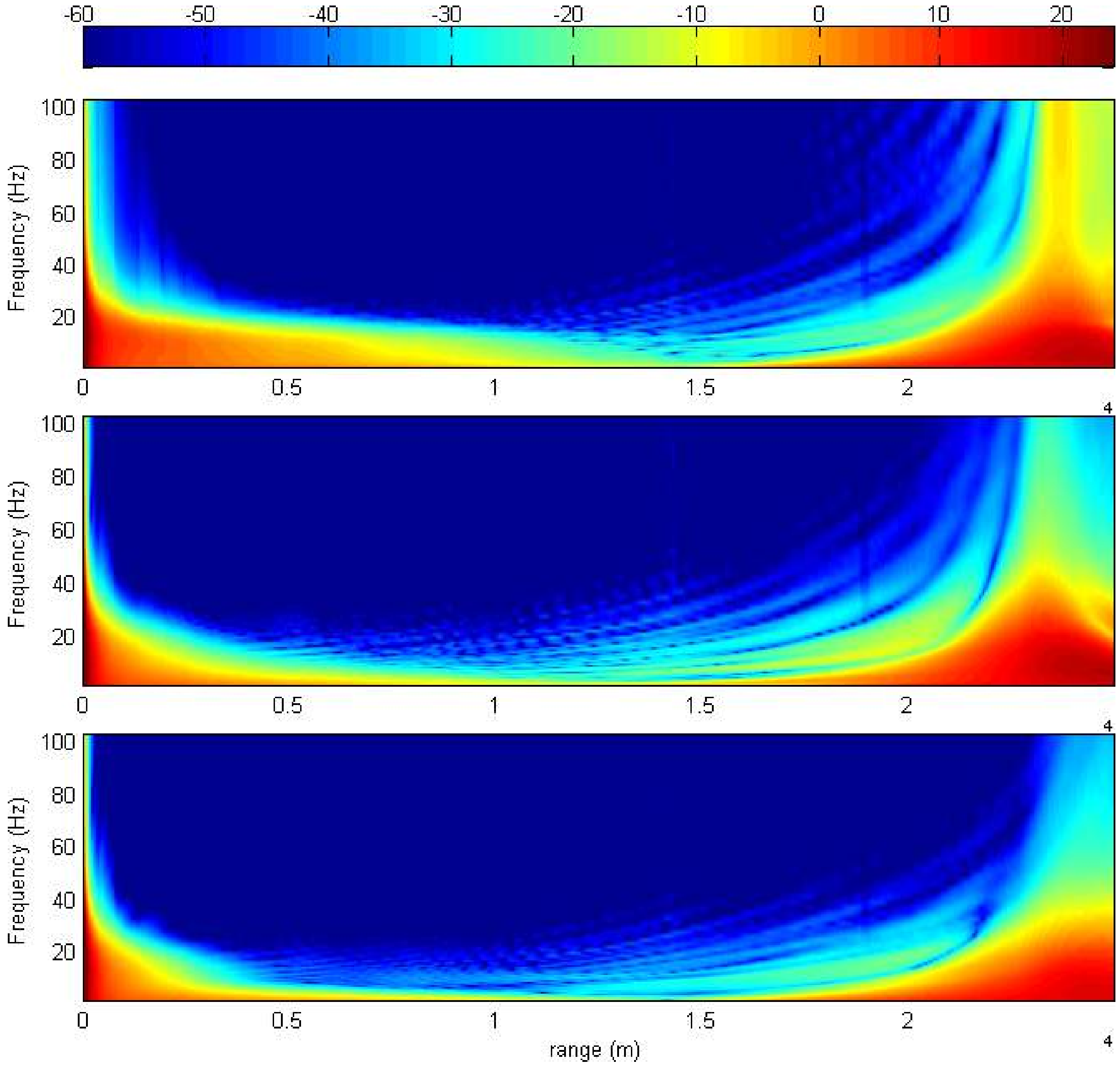

Figure 2.3: *Relative sound level as a function of range and frequency. Eastwards propagation. Top: Curve fitted profile. Middle: Full data set. Bottom: Curve fitted profile with surface taper.*

Knut Waagan. Mapping low frequency blast noise using a numerical weather forecast. Proceedings of the 38th Scandinavian Symposium on Physical Acoustics, Geilo 30 February 2 - 6, 2013. Editor: Rolf J. Korneliussen, ISBN 978-82-8123-015-6.

2 Noise prediction results

The sound source was placed at the peak in the middle of the east-west transect two meters above ground. This corresponds to the location of a military shooting range for heavy artillery, where it is necessary to control acoustic noise dispersal. Actual ground impedance data for the site was used, however real topography was not used. Instead, the topography data was dictated by the Arome output. Three different representations of the weather forecast data were used: The full data set, the range-independent curve fit, and the surface tapered curve fit.

Sound propagation from 1-100 Hz was simulated in both directions along the transect. Snapshots of the propagation simulations for 64 Hz is shown in Figure 2.1. In the westwards direction, the downwind conditions produced downward refraction from about 800 m and down. A complex pattern of reflections and interference minima can be seen, as is typical of downward refracting conditions. In the eastwards direction, sound was first refracted upwards, and then, as it reached above the jet, it was refracted downwards, reaching the ground at about 22 km range. In addition to the receding jet wind, the temperature inversion from about 1500 m altitude played a role. This refraction pattern is interesting, as it would be difficult to predict from ground based meteorological data. In the shadow region, sound level was likely underestimated, as scattering from turbulence was not taken into account. There was strong vertical variation in sound levels, however in the following we discuss only sound levels at the ground surface.

In order to compare the different weather representations, we mapped relative sound levels as functions of frequency and range, see Figures 2.2-2.3. In all cases, the combined effect of ground and weather was roughly like a low pass filter with a cut-off frequency that varied with range. The vertical lines and boundaries in the plot were due to the ground features, e.g. a lake at 7.5 km westwards.

First, we consider the westwards, i.e. downwind propagation. The range-independent curve fit mostly underestimated sound levels, especially for the higher frequencies. There was however overestimation in a low frequency band because the frequency cutoff was not so sharply defined, and the cutoff frequency was somewhat higher. Up to 12.5 km the tapered curve fit yielded remarkably similar results to the full data set. It overestimated slightly, but showed much the same features. Beyond 12.5 km there was less agreement. At the 12.5 km mark, there was a peak, beyond which more acoustic energy reaching ground had travelled above the surface layer. Hence the surface taper may have been less important. The tapered case captured the frequency cutoff all the way up 25 km. At around 22 km there was an increase in sound level, which none of the curve fit cases captured well.

The eastwards, or upwind, propagation had a very different pattern. The frequency cut-off approached zero in the refractive shadow region. Again we note that the tapered curve fit was remarkably accurate near the source. The range-independent curve fit seemed to send more low frequency energy the into shadow region, and also dampened the higher frequencies a bit more slowly. All cases captured the downward refraction effect beyond 20 km, but there were significant differences in the details.

Ground based meteorological observations are an alternative method of providing input to the PE calculation. Presently, noise mapping around this shooting range is performed utilising automatic weather stations. They are strategically situated such that a wide range of altitudes are sampled. We tried emulating this procedure by sampling the Arome data at the source location and at two locations west of the source. The effective sound speed was then assumed to vary only with altitude and interpolated linearly between the sample points. Above the highest sample point (i.e. the source location) the effective sound speed was assumed constant. For westwards (downwind) propagation, sound levels were much like the range-independent curve fit. This agreement can be explained by the absence of downward refracting conditions higher up. Eastwards on the other hand, the downward refraction effect could obviously not be modelled by weather station data alone, but the refractive shadow was clearly represented.

2.1 Summary

Before summarising, we should point out that the representativity of the weather forecast data set has not been investigated. The weather consisted of moderate winds, and temperature stratification seemingly typical of daytime conditions. Data from e.g. other times of year, and with other wind directions might give different conclusions. In particular, strong temperature inversions occur in this area in winter, which can cause large received noise levels, while being challenging for weather forecasters to predict.

The forecast data provides an opportunity to study how and whether simplified weather models can be used in noise prediction. Some of the simplified models we studied here captured the large scale patterns of the noise propagation well. Some details were lost, and this could result in large errors locally.

The importance of higher atmospheric layers for long range propagation was highlighted. On the other hand, if only the lower layers are downward refracting, or ranges are sufficently short, prediction based on near-ground observations seems feasible. The weather data featured a clear surface layer effect, and including a simple emulation of the surface layer in the sound propagation strongly improved results up to a certain distance from the source. This could be because the refractive conditions near ground influence the ground loss. We remark that the actual surface layer in this terrain is likely more complicated than the data suggests.

References

[1] F Bouttier. Arome system documentation, 19 pp, 2009.

[2] Finn Løvholt. Ground classification. *NGI report*, 2007.

[3] Christian Madshus, Finn Løvholt, Amir Kaynia, Lars Robert Hole, Keith Attenborough, and Shahram Taherzadeh. Air-ground interaction in long range propagation of low frequency sound and vibration - field tests and model verification. *Applied Acoustics*, 66(5):553–578, 2005.

[4] R.A. Sack and M. West. A parabolic equation for sound propagation in two dimensions over any smooth terrain profile: The generalised terrain parabolic equation (GT-PE). *Applied Acoustics*, 45(2):113–129, 1995-02-01T00:00:00.

[5] Knut Waagan. Low-frequency long-range atmospheric noise propagation modelling with the PE method. Technical report, Technical Report FFI/RAPPORT-2014/00260, Norwegian Defence Research Establishment, 2014.